Mon. Not. R. Astron. Soc. **361,** 1187–1196 (2005) doi:10.1111/j.1365-2966.2005.09246.x

Seismic analysis of the second ionization region of helium in the Sun – I. Sensitivity study and methodology

Mário J. P. F. G. Monteiro[1,2★] and Michael J. Thompson[3]

[1]*Centro de Astrofísica da Universidade do Porto, Rua das Estrelas, 4150-762 Porto, Portugal*
[2]*Departamento de Matemática Aplicada, Faculdade de Ciências da Universidade do Porto, Rua do Campo Alegre 687, 4169-007 Porto, Portugal*
[3]*Department of Applied Mathematics, University of Sheffield, Hicks Building, Hounsfield Road, Sheffield S3 7RH*

Accepted 2005 May 26. Received 2005 May 3; in original form 2005 February 3

ABSTRACT

The region of the second ionization of helium in the Sun is a narrow layer near the surface. Ionization induces a local change in the adiabatic exponent Γ_1, which produces a characteristic signature in the frequencies of p modes. By adapting the method developed by Monteiro, Christensen-Dalsgaard & Thompson, we propose a methodology for determining the properties of this region by studying such a signature in the frequencies of oscillation.

Using solar data we illustrate how the signal from the helium ionization zone can be isolated. Using solar models which each use different physics – the theory of convection, equation of state and low-temperature opacities – we establish how the characteristics of the signal depend on the various physical processes contributing to the structure in the ionization layer. We further discuss how the method can be used to measure the solar helium abundance in the envelope and to constrain the physics affecting this region of the Sun.

The potential usefulness of the method we propose is shown. It may complement other inversion methods developed to study the solar structure and to determine the envelope helium abundance.

Key words: equation of state – Sun: abundances – Sun: helioseismology – Sun: interior – Sun: oscillations – stars: abundances.

1 INTRODUCTION

The direct determination of the helium abundance in the solar near-surface layers is difficult and subject to uncertainty, although it is very important to the modelling of the internal structure and evolution of the Sun (see Kosovichev et al. 1992 for a comprehensive discussion of the sources of uncertainty). It is usually taken as a fitting parameter of an evolutionary sequence that provides the correct luminosity for the Sun at the present age. The ability to constrain this parameter to have the observed value for the Sun is important in order to improve the mass-loss estimates and early evolution of the Sun, as well as to test the effects of mixing and settling on stellar evolution.

Several attempts have been made to use solar seismic data to calculate the abundance of helium (Y) in the solar envelope (Dziembowski, Pamyatnykh & Sienkiewicz 1991; Vorontsov, Baturin & Pamyatnykh 1991, 1992; Christensen-Dalsgaard & Pérez Hernández 1992; Pérez Hernández & Christensen-Dalsgaard 1994; Antia & Basu 1994; Basu & Antia 1995; Gough & Vorontsov 1995; Richard et al. 1998). However, the dependence of the determination on other aspects, in particular on the equation of state, means that there are serious difficulties in obtaining an accurate direct seismic measurement of the envelope abundance of helium (Kosovichev et al. 1992; Pérez Hernández & Christensen-Dalsgaard 1994; Basu & Christensen-Dalsgaard 1997). The sensitivity of the modes to the helium abundance is primarily provided by the change of the local adiabatic sound speed c as a result of ionization. Such sensitivity is given by the behaviour of the first adiabatic exponent, Γ_1, because $c^2 \equiv \Gamma_1 p/\rho$, where p and ρ are the pressure and density respectively, and consequently the sensitivity is strongly dependent on the assumed equation of state and on other physics relevant for the region where the ionization takes place. This is the main reason why the seismic determination of the envelope abundance of helium is highly complex.

Here we propose a method complementary to those used previously, by adapting the procedure developed by Monteiro et al. (1994, hereafter MCDT) and Christensen-Dalsgaard, Monteiro & Thompson (1995, hereafter CDMT). By using the solar frequencies in a different way, and thus providing a direct probe to the region of ionization, we aim to provide a method in which the various effects at play in the ionization zone can be isolated, and therefore to construct a procedure to access the chemical abundance. Localized variations in the structure of the Sun, such as occur at the base of the convective envelope (see MCDT and Monteiro 1996) and

★E-mail: mjm@astro.up.pt (MJPFGM); Michael.Thompson@sheffield.ac.uk (MJT)

in the region of the second ionization of helium (Monteiro 1996), create a characteristic signal in the frequencies of oscillation. The properties of such a signal, as measured from the observed frequencies, are related to the location and thermodynamic properties of the layer within the Sun in which the sharp or localized variation occurs. The main advantage we see in this method is the possibility of utilizing different characteristics of the signal to distinguish different aspects of the physics of the plasma in the region where the signal is generated. In particular we may be able to separate the effects arising from convection, the low-temperature opacities and the equation of state from the quantification of the helium abundance that we seek to obtain. Here we mainly concentrate on separating these distinct contributions in order to establish the dependence of the parameters of the signal in the frequencies on the various aspects of the structure in the ionization region. Using a variational principle we determine how the zone of the second ionization of helium can indeed be considered as a localized perturbation to an otherwise 'smooth' structure, generating a characteristic signal in the frequencies of the modes.

We note that simplified versions of the expression for the signal discussed here have been applied successfully to cases in which there are only very low-degree frequencies. The signal has been fitted either to the frequencies of low-degree modes (Monteiro & Thompson 1998; Verner, Chaplin & Elsworth 2004), or to frequency differences (Miglio et al. 2003; Basu et al. 2004; Vauclair & Théado 2004; Bazot & Vauclair 2004; Piau, Ballot & Turck-Chièze 2005). Here we obtain the expression for the general case, in which there are also modes of higher degree, with the low-degree applications being a special case. We also demonstrate the method for making use of the information in moderate-degree data available only for the Sun. When using modes with degree above 4 or 5 we can avoid using frequencies affected by the base of the convection zone and may hope to achieve a much higher precision in the results, as many more frequencies with lower uncertainties can be used.

In this work we present an analysis of the characteristics of the signal under a variety of conditions. Several models containing different physics and envelope helium abundances are used to test the method in order to prepare the application to the observed solar data.

2 THE REGION OF THE SECOND IONIZATION OF HELIUM

In order to model the sensitivity of the modes to this region we must first try to understand how ionization changes the structure. Secondly, we need to estimate how the modes are affected by such a region. The details of the derivations are discussed in the Appendix, but the assumptions and the main expressions are reviewed and analysed here.

2.1 Properties of the ionization region

Because the helium second ionization zone (He II ionization zone) is sufficiently deep (well within the oscillatory region of most of the modes) we propose to adapt the method discussed in MCDT to the study of this layer. The contribution to the frequencies arising from a sharp variation in the structure of the Sun can be estimated by using a variational principle for the modes to calculate the effect due to such a localized feature. In the work by MCDT the feature was the base of the convection zone, and the sharp transition was represented by discontinuities in the derivatives of the sound speed. Because of the size of the ionization region when compared with the local wavelength of the modes, that representation is inadequate for reproducing the effect on the frequencies in the ionization region.

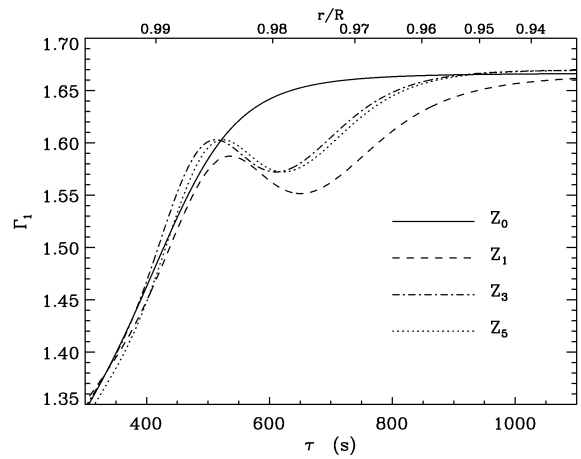

Figure 1. Plot of the adiabatic exponent Γ_1 for various solar models. As a reference we have calculated a model (Z_0) in which the second ionization of helium has been suppressed. The other three models are calculated using different equations of state. (See Table 1 for further details of the models.) The second ionization of helium takes place around an acoustic depth of 600 s, corresponding to the depression in the value of Γ_1.

Here we must, instead, consider how the ionization changes the first adiabatic exponent $\Gamma_1 \equiv (\partial \ln p/\partial \ln \rho)_s$ (the derivative at constant specific entropy s) locally, generating what can be described as a 'bump' over a region of acoustic thickness of about 300 s (see Fig. 1). This allows us to estimate how the frequencies of oscillation are 'changed' as a result of the presence of this feature in the structure of the Sun. The effect will be mainly taken into account through the changes induced in the adiabatic gradient Γ_1 by the ionization. Other thermodynamic quantities are also affected, but the changes in the local sound speed are mainly determined by changes in Γ_1. Therefore, we will calculate the dominant contribution to the changes in the frequencies by establishing the effect on the modes resulting from changes of the adiabatic exponent.

Däppen & Gough (1986) and Däppen, Gough & Thompson (1988) have proposed a method based on the same principle, using the sensitivity of the sound speed to changes in the adiabatic exponent. Using this sensitivity they calibrate a quantity that is associated with ionization in order to try to measure the helium abundance in the solar envelope from seismic data. Most methods, however, have difficulties in removing the dependence of the calibration on the physics of the reference models, making it difficult to obtain a value for the abundance. This is the problem we try to address in this contribution, by developing a method able to measure in the frequencies the effect of the ionization and its dependence on the abundance, isolated as much as possible from the other uncertainties.

2.2 A variational principle for the effect on the frequencies

A variational principle for non-radial adiabatic oscillations, assuming zero pressure at the surface located at radius R as a boundary condition, can be formulated. It is possible to consider only higher-order acoustic modes, for which we can neglect the perturbation in the gravitational potential. The outcome of such a variational principle is an estimate of how the frequencies change as a result of changes in $(\Gamma_1 p)$ and ρ. This is described and discussed in Appendix A.

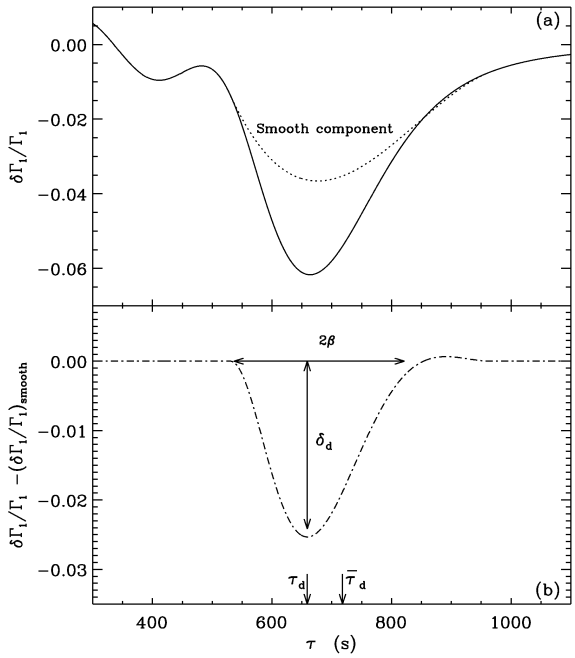

Figure 2. (a) Plot of the differences ($\delta\Gamma_1/\Gamma_1$) between two models, one with and the other without the second ionization of helium, versus the acoustic depth τ. These correspond to models Z_0 and Z_1 discussed in the text and described in Table 1. The dotted line represents our assumed smooth reference structure. (b) The change of Γ_1, relative to the smooth reference structure, is shown. The parameters represented schematically, to be determined from the characteristics of the signal in the frequencies, are: δ_d, the amplitude of the differences at τ_d; and β, the half-width of $\delta\Gamma_1/\Gamma_1$ (values taken from Table 3). Also indicated is the value of $\bar{\tau}_d$ as found from the frequencies.

In order to model the signature of the ionization zone we represent the effect of the second ionization in terms of the changes it induces in the adiabatic exponent Γ_1. Such a change (see Fig. 2) is approximately represented by a 'bump' of half-width β in acoustic depth, and relative height

$$\delta_d \equiv \left(\frac{\delta\Gamma_1}{\Gamma_1}\right)_{\tau_d}, \tag{1}$$

located at a radial position corresponding to an acoustic depth τ_d. Here, and in the following, the acoustic depth τ at a radius r is defined as

$$\tau(r) \equiv \int_r^R \frac{dr}{c}, \tag{2}$$

where R is the photospheric radius of the Sun.

Relative to the frequencies of a reference model, assumed to be 'smooth' and corresponding approximately to a model with no He II ionization region, we find that the bump changes the frequencies in such a way that there is a periodic component of the form

$$\delta\omega \sim A(\omega, l)\ \cos\Lambda_d \tag{3}$$

(see Appendix A), where the amplitude, as a function of mode frequency ω and mode degree l, is given by

$$A(\omega, l) \equiv a_0\ \frac{1-2\triangle/3}{(1-\triangle)^2}\ \frac{\sin^2[\beta\omega(1-\triangle)^{1/2}]}{\beta\omega}, \tag{4}$$

and the argument is

$$\Lambda_d \equiv 2\left[\omega\int_0^{\tau_d}(1-\triangle)^{1/2}\,d\tau + \phi\right]. \tag{5}$$

Here the factor in $\triangle$ represents the geometry of the ray path, accounting for deviation from the vertical when the mode degree is non-zero. It is associated with the Lamb frequency, as given below (equations 8 and 9). In fact, because the ionization zone is close to the surface, and provided we are not using very high-degree data, we can neglect $\triangle$ in the expression for the argument Λ_d; we can similarly neglect the effect of the mode degree on the surface phase function ϕ. Consequently, for the ionization zone the expression for the argument becomes

$$\Lambda_d \sim 2\,(\omega\tau_d + \phi) \simeq 2\,(\omega\bar{\tau}_d + \phi_0)\,. \tag{6}$$

In the asymptotic expression used for the eigenfunction (see equation A4), the phase ϕ depends on the mode frequency and degree (see MCDT for details). Here we have expanded the phase to first order in frequency, by writing $\phi(\omega) \simeq \phi_0 + a_\phi\omega$. From this it follows that $\bar{\tau}_d \equiv \tau_d + a_\phi$, while the frequency-independent term of the phase is now ϕ_0.

The amplitude of the signal is proportional to a_0, a quantity given by

$$a_0 = \frac{3\delta_d}{2\tau_t}, \tag{7}$$

where $\tau_t \equiv \tau(0)$ is the total acoustic size of the Sun. The small factor $\triangle$, present in the amplitude, is given by

$$\triangle = \triangle_d\ \frac{l(l+1)}{\tilde{l}(\tilde{l}+1)}\ \frac{\tilde{\omega}^2}{\omega^2}, \tag{8}$$

where the value of $\triangle_d$ is given by

$$\triangle_d = \frac{\tilde{l}(\tilde{l}+1)}{\tilde{\omega}^2}\left(\frac{c}{r}\right)^2_{\tau=\tau_d}, \tag{9}$$

and $\tilde{l}$ and $\tilde{\omega}$ are two reference values. These values are chosen taking into account the expected behaviour of the signal and the set of modes used, as discussed below.

In order to compare the amplitude as found for different models it is convenient to define a reference value A_d, given by

$$A_d \equiv A(\tilde{\omega}, \tilde{l}) = a_0\ \frac{1-2\triangle_d/3}{(1-\triangle_d)^2}\ \frac{\sin^2\left[\beta\tilde{\omega}\,(1-\triangle_d)^{1/2}\right]}{\beta\tilde{\omega}}. \tag{10}$$

The parameters of the signal relevant to characterizing the local properties of the ionization zone, as given in equation (3), are $\bar{\tau}_d$, β, a_0 and $\triangle_d$.

The values of $\bar{\tau}_d$ and $\triangle_d$ can be used to measure mainly the location of the ionization zone; they both vary strongly with distance to the surface. The acoustic depth is a cumulative function of the sound speed behaviour over all layers from the surface to a particular position, whereas $\triangle_d$ is a local quantity, which is not affected by the behaviour of the sound speed in the layers above the ionization zone.

The values of β and a_0 (or δ_d) are expected to be directly related to the local helium abundance, because the size of the bump will be determined by the amount of helium available to be ionized. These parameters are also expected to be strongly affected by the equation of state, and, to a lesser extent, by other aspects of the physics affecting the location of the ionization zone (τ_d). We may hope, however, to be able to use the other parameters to remove this dependence, while retaining the strong relation between the bump and the helium abundance (Y).

2.3 Measuring the signal in the frequencies

Our first goal is to find the five parameters describing the signal from the frequencies of oscillation. In order to do that we must isolate a

signature of about 1 μHz in amplitude, which is superimposed on the actual frequencies. We do so by isolating, in the frequencies, the periodic signal described by equation (3) using a non-linear least-squares iterative fit to find the best set of parameters. The method used is an adaptation of the one proposed by MCDT; for the present problem we must redefine the characteristic wavelength of the signal to be isolated (quantity λ_0 in MCDT), as it is significantly larger than for the signal from the base of the convective envelope. The parameters describing the signal (equation 3), and found by our fitting procedure, are as follows:

$$\tau_{\rm d}, \quad \phi_0, \quad a_0, \quad \triangle_{\rm d}, \quad \beta\ .$$

We choose a set of modes that cross the ionization zone, but that do not cross the base of the convection zone. By removing modes that penetrate deep into the Sun (low-degree modes), we avoid the contamination coming from the signal generated at the base of the convection zone (see MCDT). When selecting only modes of higher degree (between 45 and 100), however, it becomes necessary to include the contribution from the mode degree to the amplitude of the signal. This is the reason why it is necessary to include the parameter $\triangle_{\rm d}$ in the fitting. This parameter is not necessary when studying other stars (Monteiro & Thompson 1998; Basu et al. 2004; Piau et al. 2005), resulting in a simplified description of the expected observed behaviour. In the case of the Sun it is highly advantageous to use all available high-degree modes that cross the ionization zone.

The modes considered correspond to the ones available in solar data, having degrees and frequencies such that the lower turning point is between 0.75 and 0.95 of the solar radius. The latter limit ensures that the modes cross the ionization zone, while the former avoids contamination from the signal originating at the base of the convective envelope (see, for example, CDMT and references therein). These conditions define a set of typically about 450 modes having frequency $\omega/2\pi$ in the range [1500, 3700] μHz, and with mode degree in the range $45 \leqslant l \leqslant 100$.

As we are using only modes of high degree in this work, the reference values preferred in the fitting of the signal are

$$\tilde{l} = 100 \quad \text{and} \quad \frac{\tilde{\omega}}{2\pi} = 2000\,\mu\text{Hz}.$$

The first value is an upper limit for modes that cross beyond the ionization zone, while the value of $\tilde{\omega}$ corresponds to the frequency region in which the signal is better defined. These values are only relevant for normalizing the parameters fitted for different models.

For solar observations, only frequencies with a quoted observational error of below 0.5 μHz are included. We ensure consistency of the data sets by restricting the selection of mode frequencies from the models to the modes present in the solar data after applying the above selection rules.

We stress that the method adopted for removing the smooth component of the frequencies is a key assumption in the process of fitting the signal. Here we use a polynomial fit with a smoothing parameter on the third derivative (see CDMT). In any case, as long as the analyses for the different models and for the solar data are consistent, the comparison of the parameters will be independent of the choice of how to describe the smooth component. Such consistency is ensured by using exactly the same set of frequencies and the same numerical parameters for the fitting for each model.

2.4 The signal in the solar data

To illustrate the signal extraction, the method proposed here was applied to an analysis of solar seismic data from MDI on the *SOHO* spacecraft (Scherrer et al. 1995). The signal was isolated as described above for the models. The fitted signal of the Sun is shown in Fig. 3(a), together with the error bars. In order to illustrate how well the expression for the signal (equation 3) fits the data points we show in Fig. 3(b) the signal in the frequencies normalized by the amplitude as given in equation (4). The quality of the fit done with equation (3) confirms the adequacy of the first-order analysis developed in Appendix A leading to the expression given by equation (4).

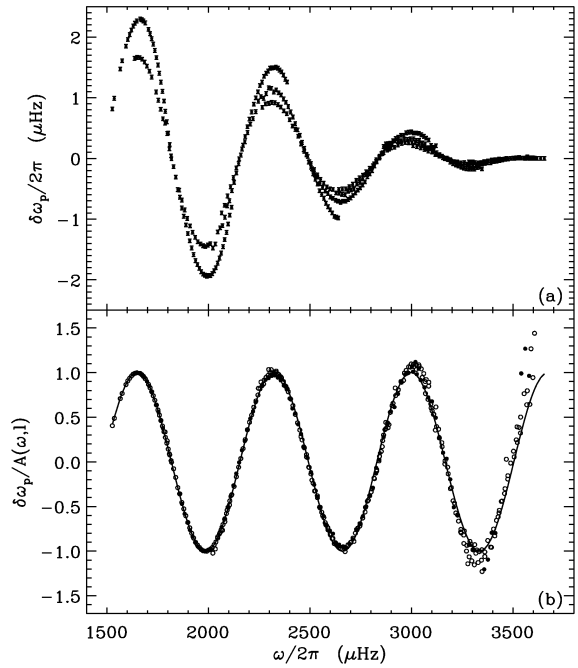

Figure 3. (a) Residuals left after a smooth component of the frequencies, as a function of mode order and degree, is removed. The data are from MDI/SoHO, with the error bars corresponding to a 3σ of the quoted observational errors. (b) Plot of the signal isolated, and shown in panel (a), after division by the amplitude function as given by equation (4) when using the values of $(a_0, \delta_{\rm d}, \beta, \triangle_{\rm d})$ found in the fitting. Modes with degree below $l = 60$ are shown as filled circles, while modes with a higher value of the degree are represented by open circles. The line indicates the fitted periodic signal as expected from equation (3).

The values of the parameters found for the data are given in Table 1. From Monte Carlo simulations we have estimated the uncertainty in the determination of the parameters resulting from observational uncertainties, as indicated by the quoted observational errors. The values found, at the 3σ level, are also listed in Table 1. It is clear that, as a result of the large amplitude of this signature (above 1 μHz at $\omega/2\pi = 2000$ μHz), the precision with which the parameters are determined is very high. As long as the method to isolate this characteristic signature is able to remove the 'smooth' component, the results can be used with great advantage for analysing the zone of the second ionization of helium in the Sun.

3 SOLAR MODELS WITH DIFFERENT PHYSICS

In order to establish how sensitive the various characteristics of the signal are to the properties of the ionization zone, and therefore to the aspects of the Sun that affect the ionization zone, we consider various static models of the Sun calculated with the same mass, photospheric

Table 1. Parameters obtained by fitting the observed solar frequency data with the expression for the signal as given in equation (3). The quantities τ_d and β are given in seconds, while the amplitudes (a_0 and A_d) are given in μHz. Note that A_d is not a fitting parameter, as it is derived from the other parameters using equation (10). The standard deviations σ are estimated from 200 simulations of the effect of the observational uncertainties on the determination of the parameters.

	$\bar{\tau}_d$	ϕ_0	$a_0/2\pi$	$A_d/2\pi$	β	$\triangle_d$
Sun	741.2	1.743	1.987	2.655	141.3	0.493
3σ	1.9	0.027	0.056	0.037	0.96	0.015

radius and luminosity. The profile of the helium abundance in the models is obtained by calibrating with a constant factor a prescribed abundance profile from an evolution model with the age of the Sun (without settling).

We note that the imposition of the same radius and luminosity for all models is the key difference between the analysis presented here and the work by Basu et al. (2004). If the models are not required to have the same luminosity and radius as the Sun, the properties of the ionization zone are not affected in the same way. Consequently, the behaviour of the amplitude of the signal in this case is different from what we find when the above two conditions are imposed on the models.

The aspects of the physics being tested here are the *equation of state (EoS)*, the *theory of convection* and the *opacity*. All these aspects affect the ionization zone by changing its location, size and thermodynamic properties.

All models were calculated as in Monteiro (1996; see also Monteiro, Christensen-Dalsgaard & Thompson 1996). These are not intended to give an accurate representation of the Sun, but simply to illustrate the usefulness of the method we propose in the study of a particular region of the solar envelope.

As the simplest possible EoS we have used a Saha equation of state with full ionization at high pressure – this corresponds to SEoS in Table 2. As a more complete EoS we have used the CEFF equation of state as described in Christensen-Dalsgaard & Däppen (1992). For the opacities we have considered a simple power-law fit (SOp), or the Rosseland mean opacity tables at low temperatures from Kurucz (1991). To include convection we have taken the standard mixing-length theory (Böhm-Vitense 1958, parametrized as in Monteiro et al. 1996) or the more recent CGM model (Canuto, Goldman & Mazzitelli 1996).

Table 2. Solar models and their helium (Y) abundances. Also indicated are the equation of state (EoS): SEoS – Simple Saha equation of state with pressure ionization, and CEFF (cf. Christensen-Dalsgaard & Däppen 1992); the opacity: SOp – simple power-law fit of the opacities, and Kur – low-temperature opacities from Kurucz (1991); and the formulation for modelling convection: MLT – standard mixing-length theory (Böhm-Vitense 1958, parametrized as in Monteiro et al. 1996), and CGM – Canuto et al. (1996). See the text for a description of the parameter f_ϵ used in the calculation of the emissivity.

Model	EoS	Opacity	Convection	Y	f_ϵ
Z_0	SEoS	SOp	MLT	0.24615	
Z_1	SEoS	SOp	MLT	0.24608	
Z_2	SEoS	SOp	CGM	0.24608	
Z_{3l}	CEFF	SOp	MLT	0.24149	0.8
Z_3	CEFF	SOp	MLT	0.24981	
Z_{3h}	CEFF	SOp	MLT	0.25667	1.2
Z_4	CEFF	SOp	CGM	0.24981	
Z_{5l}	CEFF	Kur	MLT	0.24148	0.8
Z_5	CEFF	Kur	MLT	0.24980	
Z_{5h}	CEFF	Kur	MLT	0.25667	1.2
Z_{5v}	CEFF	Kur	MLT	0.26246	1.4
Z_6	CEFF	Kur	CGM	0.24980	

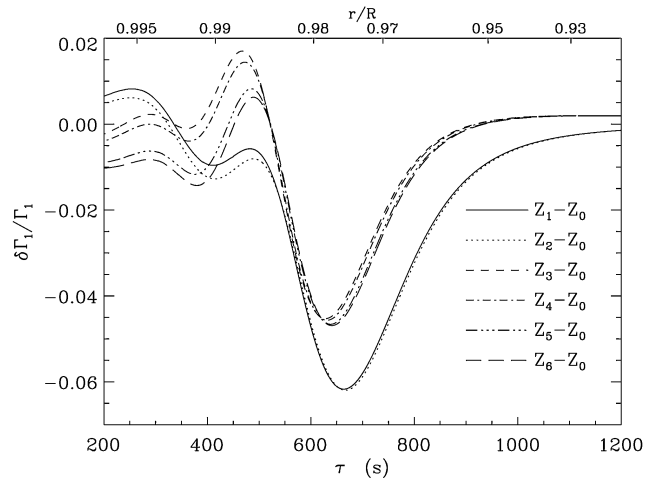

Figure 4. Plot of the difference in Γ_1 between each model considered and the model without the second ionization of helium. See Table 2 for the details of each model. Only the region around the second ionization of helium is shown, corresponding to the negative bump around an acoustic depth of 650 s.

The behaviour of the adiabatic exponent for some of the models (see Table 2), relative to our reference model (Z_0), is illustrated in Fig. 4. There is a clear difference in the location of the ionization zone (τ_d) when a different EoS is used. The effects of changes in the formulation of convection or in the opacities are much smaller.

In order to have models with the same envelope physics, but different helium abundances, we have calculated solar models with the energy generation rate changed by a prescribed factor f_ϵ in the emissivity. These are models $Z_{3l,3h}$ and $Z_{5l,5h,5v}$, which are similar to Z_3 and Z_5, respectively, except for the value of f_ϵ, which is now different from unity. These models have different core structures, but envelopes with exactly the same set of physics. All differences between these models in the envelope arise from differences in the chemical composition. To illustrate the differences we plot in Fig. 5 the differences in Γ_1 between models with the same physics but increasing values for the envelope abundance of helium. As the helium abundance increases, there is a corresponding decrease in hydrogen, which results in a slight separation in temperature of the three major ionization regions. Consequently, both ionization regions for the helium expand towards higher temperatures. As the bump becomes slightly wider and moves to a higher temperature, the effect on the frequencies is expected to become smaller.

For all models we have calculated the frequencies of linear adiabatic oscillations. The set of frequencies for each model, as used to fit the signature of the ionization zone, is described above.

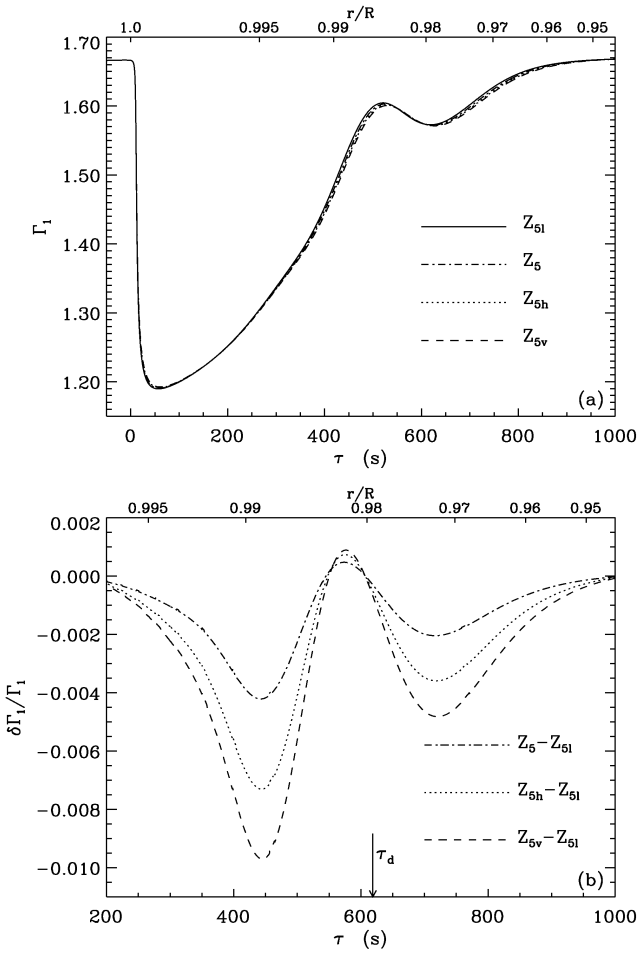

Figure 5. (a) Plot of the adiabatic exponent Γ_1 for all models '5', calculated with the same physics but different surface helium abundances as imposed by f_ϵ (see Table 2). The hydrogen and both helium ionization regions are shown. (b) Plot of the differences in Γ_1 between models $Z_{5,\,5h,\,5v}$ and model Z_{5l}. See Table 2 for the details of each model. Only the region around the second ionization of helium (indicated by the arrow) is shown.

The parameters obtained in fitting equation (3) to the frequencies of the models listed in Table 2 (excluding Z_0) are given in Table 3.

4 THE EFFECT OF THE PHYSICS ON THE CHARACTERISTICS OF THE SIGNAL

The set of solar models considered here, and listed in Table 2, covers three major aspects of the physics that determines the surface structure of the models, namely the equation of state, the low-temperature opacities, and the formulation for convection (defining the superadiabatic layer). In order to use the diagnostic potential of this characteristic signature (as given by equation 3) in the frequencies we need to understand how each parameter describing the signal is affected by a specific aspect of the physics defining the structure of the envelope.

One would expect the shape of the bump to be strongly determined by the EoS. However, any change in the structure that affects the location of the ionization zone will necessarily affect the characteristics of the Γ_1 profile. Consequently, we need first to identify the parameters that depend more strongly on the location – namely $\bar{\tau}_\mathrm{d}$ and $\triangle_\mathrm{d}$.

Table 3. Parameters obtained by fitting the frequency data for the models with the expression for the signal as given in equation (3). The quantities τ_d and β are given in seconds, while the amplitudes (a_0 and A_d) are given in μHz. Note that A_d is not a fitting parameter, as it is derived from the other parameters using equation (10).

Model	$\bar{\tau}_\mathrm{d}$	ϕ_0	$a_0/2\pi$	$A_\mathrm{d}/2\pi$	β	$\triangle_\mathrm{d}$
Z_1	718.0	2.588	1.634	2.834	142.5	0.604
Z_2	724.8	2.525	1.671	2.862	141.9	0.599
Z_{3l}	729.9	1.950	2.500	3.251	146.0	0.484
Z_3	730.4	1.951	2.380	3.140	144.7	0.490
Z_{3h}	730.4	1.951	2.314	3.066	144.3	0.491
Z_4	739.9	1.859	2.353	3.151	143.3	0.495
Z_{5l}	737.7	1.874	2.429	3.241	143.7	0.494
Z_5	737.8	1.876	2.342	3.145	143.1	0.496
Z_{5h}	737.5	1.880	2.278	3.072	142.7	0.498
Z_{5v}	736.8	1.890	2.205	3.002	141.7	0.502
Z_6	746.4	1.790	2.280	3.141	141.3	0.507

The changes in the upper structure of the envelope are expected to have a direct effect on the turning point of the modes. Consequently, we need to look at the parameters that may be affected by the upper reflecting boundary – in particular ϕ_0.

Finally, the area of the bump in Γ_1 in the ionization zone should reflect the local abundance of helium, if the location is well defined. Therefore we will look at a_0 and β in order to identify how the helium abundance Y defines the characteristics of the signal in the frequencies.

4.1 The location of the ionization zone

The most easily identifiable characteristic of the signal is its period. This quantity depends strongly on τ_d, but, as discussed when deriving equation (6), the period also contains a contribution from the upper turning point of the modes (where there is a phase shift of the eigenfunction). This means that the period, or, more precisely, $\bar{\tau}_\mathrm{d}$, that we measure is not necessarily a good estimate of the location τ_d of the ionization zone.

Fig. 6(a) shows the value of $\bar{\tau}_\mathrm{d}$, as found from fitting the signal in the frequencies, versus the value of τ_d as determined from the location of the local minimum of Γ_1 in the model. There is a difference of up to about 140 s between $\bar{\tau}_\mathrm{d}$ and τ_d, and one is not simply a function of the other. The difference between the two comes from a_ϕ, which measures the leading-order frequency dependence of the phase transition that the eigenfunctions undergo at the upper turning point. This will be strongly affected by the aspects of the physics that change the structure of the surface, namely convection, EoS, the low-temperature opacities, and the structure of the atmosphere. Consequently, we have to use some caution when taking the parameter $\bar{\tau}_\mathrm{d}$ from the fit to estimate the location of the ionization region.

As an alternative, it is possible to consider one of the other parameters that depend on the position of the ionization zone, namely $\triangle_\mathrm{d}$. This parameter is given in Table 3 for all models and shown in Fig. 6(b) as a function of the actual acoustic location of the ionization region. The value of $\triangle_\mathrm{d}$, defined in equation (9), is not sensitive to the layers near the photosphere, as its value is determined exclusively by the sound speed at the ionization zone. However, the determination of this term is associated with a small correction in the amplitude, which makes it more sensitive to the observational errors when fitting the frequencies.

Both panels in Fig. 6 show the solar values of $\bar{\tau}_\mathrm{d}$ and $\triangle_\mathrm{d}$ with 3σ uncertainties. The values of $\triangle_\mathrm{d}$ indicate that all models calculated

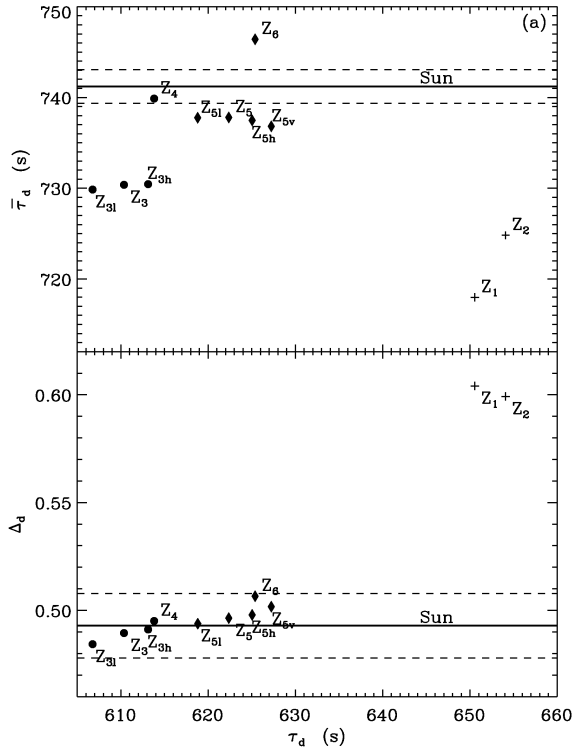

Figure 6. Plot of (a) the fitted acoustic depth $\bar{\tau}_d$ and (b) the correction term $\triangle_d$ versus the acoustic depth τ_d as determined from the models and corresponding to the local minimum in Γ_1 (see Fig. 1). Filled symbols are for models using the CEFF equation of state, while crosses are for models calculated using a simple Saha equation of state. The filled circles are for models having the same simple opacity (power law) but different theories of convection, while the filled diamonds are for models in which the opacity at low temperatures is from Kurucz. The values found for the solar data are also shown in both panels, with 3σ error bars (dashed horizontal lines) resulting from the observational uncertainties.

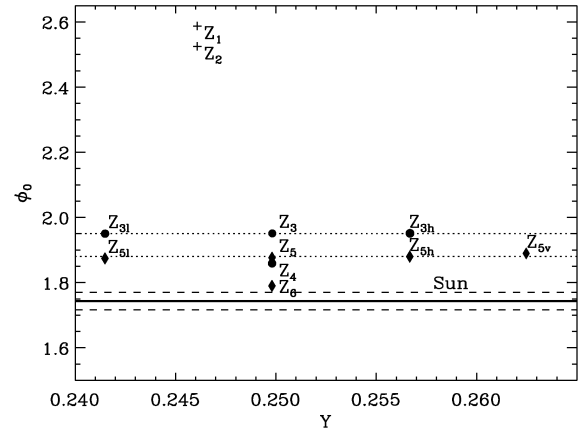

Figure 7. Plot of the phase ϕ_0 of the signal versus the envelope helium abundance Y for all models. The symbols are the same as in Fig. 6. The dotted lines illustrate the correlation among models with the same physics but different values of the surface helium abundance Y. The value found for the solar data is also shown, with 3σ error bars (dashed horizontal lines) resulting from the observational uncertainties.

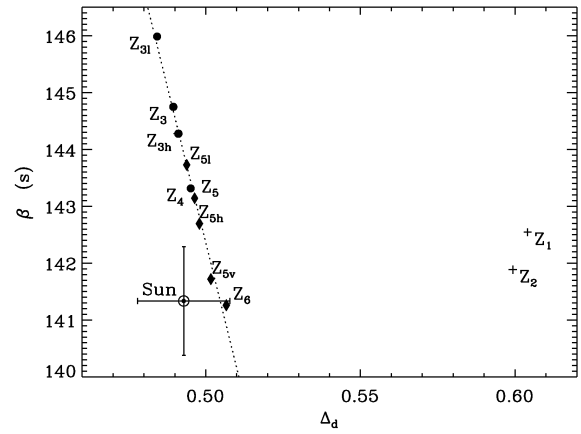

Figure 8. Plot of the estimated width of the bump, as given by β, versus the value of $\triangle_d$, providing an indication of the location of the ionization zone. The symbols are the same as in Fig. 6. The dashed line indicates a linear fit to the models with the same EoS. The values found for the solar data are also shown, with 3σ error bars resulting from the observational uncertainties.

with the CEFF equation of state give, even if only marginally, a location for the ionization zone consistent with the Sun.

Finally, the structure at the top of the envelope is also expected to be reflected in the value of ϕ_0. The value of this parameter for all models is represented in Fig. 7 as a function of the envelope helium abundance. The largest difference is found when changing the EoS (about 0.06). Changes in the opacities change ϕ_0, by as much as 0.01, while the theory of convection changes this by about 0.01. It is interesting to confirm that the fitted value of ϕ_0 is independent of the helium abundance, as one would expect from the analysis leading to the expression for the signal. Consequently, ϕ_0 may allow a separation between the helium abundance and the physics relevant to the outer layers of the Sun, because it is insensitive to Y whilst being indicative of some near-surface change that may be required in the physics.

The solar value for ϕ_0 is also shown in Fig. 7. Adjustments in the near-surface layers seem to be necessary in order to produce models that have a value of ϕ_0 consistent with the Sun. Changes in the superadiabatic layer or in the surface opacities may be some of the options available for reconciling the models with the solar data.

4.2 The equation of state

From the analysis of the results listed in Table 3, and as discussed in the previous section, the EoS is the most important factor in defining the characteristics of the signal. In Fig. 8 we show the width parameter β as a function of $\triangle_d$ (a proxy for the location). Models that have the same EoS (CEFF) lie on a common locus in this diagram, as indicated by the dotted line. The position along this line of models built with the CEFF varies according to changes in the convection or the surface opacities. Models Z_1 and Z_2, built with a different EoS, lie in a different region of the diagram. Thus we claim that, with the location of the ionization zone fixed, the width of the bump in Γ_1 is mainly a function of the EoS, as expected.

Consequently, after using ϕ_0 to test the surface physics, it is possible to combine the constraints provided by $\triangle_d$ and β to obtain a direct test on the EoS and the location of the ionization zone.

Fig. 8 also includes the parameters found for the solar data. These are marginally consistent with the expected behaviour found using models calculated with the CEFF equation of state. Other options for the EoS must be considered in order to make the models more consistent with the Sun.

4.3 The helium abundance in the envelope

From the discussion in the previous sections it follows that any determination of the helium abundance requires a careful tuning of the models to the correct structure of the envelope. Such a fine tuning can be performed based on the sensitivity of the eigenfrequencies to the behaviour of the adiabatic exponent in the region where helium undergoes its second ionization. Note, as discussed above, the following points.

(i) $\triangle_{\rm d}$ provides a process to place the ionization zone in the model at the same acoustic depth as for the Sun. This corresponds to adapting mainly the surface layers of the model (atmosphere and/or convection) in order to place the ionization zone at the same acoustic location as measured in the Sun by the solar value of $\triangle_{\rm d}$.

(ii) β can then be used to adjust the EoS (or more probably to select it from a few candidates) to match the observed behaviour. This corresponds to verifying that the behaviour of β as a function of the location ($\triangle_{\rm d}$) in the models includes the observed solar values for these two parameters.

(iii) Finally, the parameters $\bar{\tau}_{\rm d}$ and ϕ_0 can be combined to adjust the surface physics in the model, in order to recover the observed solar values. This corresponds to adjusting the convection (superadiabatic region, mainly), opacities (low-temperature range), photosphere, etc., in a complementary way to that which is carried out in point (i), until the solar values can be recovered with the models. Note that both parameters are strongly dependent on these aspects of the physics, but quite insensitive to the actual helium abundance.

Consequently, we are left with one last parameter, connected to the shape of the bump through $\delta_{\rm d}$, which is the amplitude of the signal a_0, or $A_{\rm d}$. If the model has been adjusted to the observed data using the remaining parameters, the amplitude will depend mainly on the helium abundance in the model, which can now be compared with the solar abundance. Such a relation provides a measurement of the helium abundance, which complements the boundary condition used in the evolution to fit the model to the present-day Sun.

Fig. 9 illustrates how such a dependence of $A_{\rm d}$, as defined in equation (10), could be constructed after the other aspects of the physics have been adjusted. It is worth noting that, as expected from Fig. 5, the amplitude *decreases* with increasing Y, since the changes in Γ_1 resulting from changes in the hydrogen abundance dominate the variations of the bump. This regime for the inverse dependence of the amplitude of the signal on the abundance of helium is relevant for stars of low effective temperature. This follows from the overlapping of the three ionization zones (H I, He I, He II). For stars in which these are fully separated in temperature it is expected that the amplitude will *increase* with the abundance of helium.

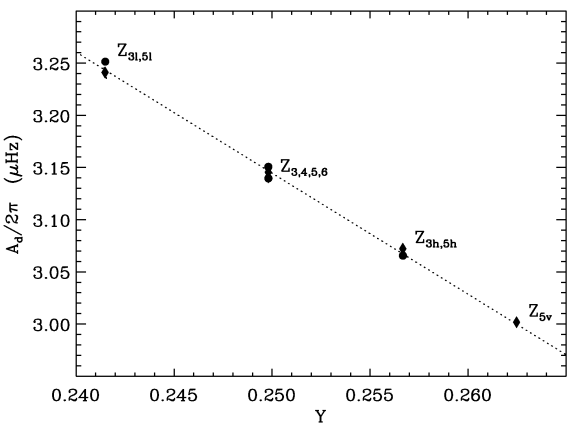

Figure 9. Plot of the reference amplitude (see equation 10) versus the envelope helium abundance Y. The symbols are the same as in Fig. 6. The dotted line illustrates the correlation between the helium abundance Y and the amplitude.

As shown above (see Figs 7 and 8), the models used here are not fully consistent with the physics of the Sun, and seem to be only marginally consistent regarding the equation of state that has been used. Consequently, the amplitude $A_{\rm d}$, as found for the solar data, cannot yet be used as an indicator of the helium abundance in the solar envelope. A more adequate calibration of the surface layers in the models must be developed before an estimation for Y is inferred from this parameter.

The simplified models that we are using here to illustrate the applicability of the method have been calculated by scaling a chemical profile determined without including diffusion and the settling of helium. This is one of the aspects that needs to be considered in order to adjust the parameters of the signal for the models to the solar values. With such a tuning, based on other seismic constraints and on the parameters of the signal discussed here, we have an independent procedure to adjust our models to the Sun in this region near the surface, where the uncertainties in the physics dominate the structure of the models.

5 CONCLUSION

In this work we have developed a method to constrain the properties of the helium second ionization region near the surface of the Sun using high-degree mode frequencies. The method is complementary to other inversion methods already available and can independently test properties of this region, and provides a possible direct measurement of the helium abundance in the envelope.

We have shown that some of the parameters characterizing the signature in the frequencies arising from this region in the Sun are very sensitive to the EoS used in the calculation of the models, and so can be used to test and constrain the EoS. Other parameters can also provide an important test on the physics affecting the surface regions of the models, namely convection and the low-temperature opacities. By combining the diagnostic potential of the five parameters determined from the data with very high precision, the helium abundance can be effectively constrained.

Here our main concern was to establish the method and demonstrate how it can be used to study the He II ionization zone in the Sun, and the physics that affect the structure of the Sun in that region. In spite of having used simplified models to represent the Sun we have illustrated the sensitivity of each parameter to the physics, establishing an approach that can be followed when adequate up-to-date evolved solar models are used. In addition to the physical ingredients addressed here, aspects such as diffusion and settling and improved opacities have to be implemented in order to provide a physically consistent value of the helium abundance. A calibration of the actual solar helium abundance using models with the best up-to-date physics will be the subject of the second paper in this series.

ACKNOWLEDGMENTS

We are grateful to S. Basu, J. Christensen-Dalsgaard, M. P. di Mauro and A. Miglio for valuable discussions. This work was supported in part by the Portuguese Fundação para a Ciência e a Tecnologia through projects POCTI/FNU/43658/2001 and POCTI/

CTE-AST/57610/2004 from POCTI, with funds from the European programme FEDER.

REFERENCES

Antia H. M., Basu S., 1994, ApJ, 426, 801
Basu S., Antia H. M., 1995, MNRAS, 276, 1402
Basu S., Christensen-Dalsgaard J., 1997, A&A, 322, L5
Basu S., Mazumdar A., Antia H. M., Demarque P., 2004, MNRAS, 350, 277
Bazot M., Vauclair S., 2004, A&A, 427, 965
Böhm-Vitense E., 1958, Zs Ap, 46, 108
Canuto V. M., Goldman I., Mazzitelli I., 1996, ApJ, 473, 550
Christensen-Dalsgaard J., Däppen W., 1992, A&AR, 4, 267
Christensen-Dalsgaard J., Péréz-Hernández F., 1992, MNRAS, 257, 62
Christensen-Dalsgaard J., Monteiro M. J. P. F. G., Thompson M. J., 1995, MNRAS, 276, 283 (CDMT)
Däppen W., Gough D. O., 1986, in Gough D. O., ed., Seismology of the Sun and the Distant Stars. NATO ASI, Reidel, Dordrecht, p. 275
Däppen W., Gough D. O., Thompson M. J., 1988, in Domingo V., Rolfe E.J., eds, Proc. ESA Symp. 286, Seismology of the Sun and Sun-like Stars. EAS, Nordwijk, p. 505
Dziembowski W. A., Pamyatnykh A. A., Sienkiewicz R., 1991, MNRAS, 249, 602
Gough D. O., Vorontsov S. V., 1995, MNRAS, 273, 573
Kosovichev A. G., Christensen-Dalsgaard J., Däppen W., Dziembowski W. A., Gough D. O., Thompson M. J., 1992, MNRAS, 259, 536
Kurucz R. L., 1991, in Crivellari L., Hubeny I., Hummer D. G., eds, Stellar Atmospheres: Beyond Classical Models. NATO ASI Series, Kluwer, Dordrecht, p. 441
Miglio A., Christensen-Dalsgaard J., Di Mauro M. P., Monteiro M. J. P. F. G., Thompson M. J., 2003, in Thompson M. J., Cunha M. S., Monteiro M. J. P. F. G., eds, Asteroseismology Across the HR Diagram. Kluwer, Dordrecht, p. 537
Monteiro M. J. P. F. G., 1996, PhD thesis, Queen Mary and Westfield College, Univ. London
Monteiro M. J. P. F. G., Thompson M. J., 1998, in Deubner F.-L., Christensen-Dalsgaard J., Kurtz D. W., eds, Proc. IAU Symp. 185, New Eyes to See Inside the Sun and Stars. Kluwer, Dordrecht, p. 819
Monteiro M. J. P. F. G., Christensen-Dalsgaard J., Thompson M. J., 1994, A&A, 283, 247 (MCDT)
Monteiro M. J. P. F. G., Christensen-Dalsgaard J., Thompson M. J., 1996, A&A, 307, 624
Pérez Hernández F., Christensen-Dalsgaard J., 1994, MNRAS, 269, 475
Piau L., Ballot J., Turck-Chièze S., 2005, A&A, 430, 571
Richard O., Dziembowski W. A., Sienkiewicz R., Goode P. R., 1998, A&A, 338, 756
Scherrer P. H. et al., 1995, Sol. Phys., 162, 129
Vauclair S., Théado S., 2004, A&A, 425, 179
Verner G. A., Chaplin W. J., Elsworth Y., 2004, MNRAS, 351, 311
Vorontsov S. V., Baturin V. A., Pamyatnykh A. A., 1991, Nat, 349, 49
Vorontsov S. V., Baturin V. A., Pamyatnykh A. A., 1992, MNRAS, 257, 32

APPENDIX A: A VARIATIONAL PRINCIPLE FOR THE HE II IONIZATION ZONE

We consider here a variational principle, following the procedure of Monteiro (1996), for describing how the modes are affected by the presence of the region of the second ionization of helium. We start by using a variational principle, for small changes of the eigenfrequencies (ω) arising from small changes of the structure. It can be written (see Christensen-Dalsgaard et al. 1995, and references therein) in the form

$$\delta\omega^2 = \frac{\delta I}{I_1}, \qquad \text{with} \qquad I_1 \sim \frac{1}{2}\,\tau_{\rm t} E_o^2\,. \tag{A1}$$

Here, $\tau_{\rm t}$ is the acoustic size of the Sun, and

$$\delta I \sim \int_0^{\tau_{\rm t}} \left[\left(\delta B_1 + \frac{{\rm d}\delta B_0}{{\rm d}\tau} \right) E_r^2 + \delta B_2 \, \frac{{\rm d}E_r^2}{{\rm d}\tau} + \delta B_3 \, \frac{{\rm d}^2 E_r^2}{{\rm d}\tau^2} \right] {\rm d}\tau, \tag{A2}$$

where E_r is the normalized radial component of the eigenfunction (with constant amplitude E_0). The acoustic depth τ is defined in equation (2).

From asymptotic analysis (see MCDT) we also have that, well inside the turning points and for moderate-degree modes,

$$\frac{{\rm d}^2 E_r}{{\rm d}\tau^2} \sim -\omega^2 (1-\triangle)\; E_r, \tag{A3}$$

or

$$E_r \sim E_0 \cos\left[\omega \int_0^{\tau} (1-\triangle)^{1/2}\, {\rm d}\tau + \phi \right]. \tag{A4}$$

The changes in the structure relative to the reference ('smooth') model are described with the functions δB_i, as given by

$$\frac{\delta B_0}{g/c} = -\frac{\delta\rho}{\rho}, \tag{A5}$$

$$\begin{aligned} \frac{\delta B_1}{\omega^2} = & \left[-\frac{1}{1-\triangle} + 2\triangle_\rho - 2\,\frac{1-3\triangle/2}{(1-\triangle)^2}\,(\triangle_\rho - \triangle_c) \right. \\ & - \frac{1}{(1-\triangle)^2}\,\frac{(\triangle_\rho - \triangle_c)^2}{4\triangle_g} \\ & \left. + 2\triangle_g\,\frac{\triangle(1-3\triangle/2)}{(1-\triangle)^2} \right] \frac{\delta(\Gamma_1 P)}{(\Gamma_1 P)} \\ & + \left[\frac{1}{1-\triangle} - \triangle_\rho + \frac{1-2\triangle}{(1-\triangle)^2}\,(\triangle_\rho - \triangle_c) \right. \\ & + \frac{\triangle}{(1-\triangle)^2}\,\frac{(\triangle_\rho - \triangle_c)^2}{4\triangle_g} \\ & \left. - \triangle_g\,\frac{\triangle(1-2\triangle)}{(1-\triangle)^2} \right] \frac{\delta\rho}{\rho}, \end{aligned} \tag{A6}$$

$$\begin{aligned} \frac{\delta B_2}{g/c} = & \left[-2\,\frac{1-3\triangle/2}{(1-\triangle)^2} + \frac{1-\triangle}{2(1-\triangle)^2}\,\frac{\triangle_\rho - \triangle_c}{2\triangle_g} \right] \frac{\delta(\Gamma_1 P)}{(\Gamma_1 P)} \\ & + \left[\frac{1-2\triangle}{(1-\triangle)^2} + \frac{\triangle}{(1-\triangle)^2}\,\frac{\triangle_\rho - \triangle_c}{2\triangle_g} \right] \frac{\delta\rho}{\rho}, \end{aligned} \tag{A7}$$

and

$$\delta B_3 = \frac{1}{2}\,\frac{1}{1-\triangle}\,\frac{\delta(\Gamma_1 P)}{(\Gamma_1 P)} + \frac{1}{2}\,\frac{\triangle}{(1-\triangle)^2}\,\frac{\delta\rho}{\rho}. \tag{A8}$$

where r, ρ, c and g are the distance from the centre, density, adiabatic sound speed and gravitational acceleration, respectively. We have also introduced the following quantities:

$$\triangle = \frac{l(l+1)c^2}{r^2\omega^2}, \tag{A9}$$

where l is the mode degree, and

$$\triangle_\rho = \frac{g}{\omega^2 c}\,\frac{\rm d}{{\rm d}\tau}\log\left(\frac{g}{\rho c}\right), \tag{A10}$$

$$\triangle_c = \frac{g}{\omega^2 c}\,\frac{\rm d}{{\rm d}\tau}\log\left(\frac{g}{r^2}\right), \tag{A11}$$

$$\triangle_g = \left(\frac{g}{\omega c}\right)^2. \tag{A12}$$

These are all first-order quantities, compared with unity, because well inside the resonance cavity of the modes the local wavelength is significantly smaller than the scale of variations of the equilibrium quantities.

In order to use the expression for δI from equation (A2), it is necessary to replace the term in $(\mathrm{d}\delta B_0/\mathrm{d}\tau)$ by integrating by parts to obtain the following expression:

$$\delta I = \int_{\tau_a}^{\tau_b} \left[\delta B_1 E_r^2 + (\delta B_2 + \delta B_0) \frac{\mathrm{d}E_r^2}{\mathrm{d}\tau} + \delta B_3 \frac{\mathrm{d}^2 E_r^2}{\mathrm{d}\tau^2} \right] \mathrm{d}\tau. \tag{A13}$$

The integration is done only for the region of the ionization zone, starting at τ_a and ending at τ_b. Because we are restricting our analysis to localized variations, it is assumed that the model differences are zero everywhere else. This does not affect our result since we will only take those changes in the frequencies that are not affected by model differences spreading over regions of size of the order of (or larger than) the local wavelength of the modes.

We recall, from asymptotic analysis, that

$$\begin{aligned} E_r^2 &\sim \frac{E_o^2}{2} \cos(\Lambda), \\ \frac{\mathrm{d}E_r^2}{\mathrm{d}\tau} &\sim -\frac{E_0^2}{2} 2\omega(1-\triangle)^{1/2} \sin(\Lambda), \\ \frac{\mathrm{d}^2 E_r^2}{\mathrm{d}\tau^2} &\sim -\frac{E_0^2}{2} 4\omega^2(1-\triangle) \cos(\Lambda). \end{aligned} \tag{A14}$$

The argument of the trigonometric functions is

$$\Lambda(\tau) \equiv 2 \left[\omega \int_0^{\tau} (1-\triangle)^{1/2} \mathrm{d}\tau + \phi \right] . \tag{A15}$$

After replacing these expressions in the equation for δI, we find that

$$\frac{2}{\omega^2 E_o^2} \delta I \sim \int_{\tau_a}^{\tau_b} \left\{ \left[\frac{\delta B_1}{\omega^2} - 4(1-\triangle)\delta B_3 \right] \cos\Lambda - 2(1-\triangle)^{1/2} \frac{\delta B_2 + \delta B_0}{\omega} \sin\Lambda \right\} \mathrm{d}\tau. \tag{A16}$$

This expression gives the variational principle for perturbations in the frequencies arising from small changes in the structure, as described by δB_i.

The next step is to establish the effect on the structure of the ionization zone for helium, relative to a model in which such a localized effect is not present. In particular, we need to estimate how Γ_1, P and ρ are changed from being slowly varying functions of depth to the actual values they have when the second ionization of helium occurs. The difference will produce the $\delta(\Gamma_1 P)$ and $\delta\rho$ responsible for changing the frequencies, as given in equations (A5–A8). This will allow us to calculate an expression for the characteristic signal we want to isolate in the frequencies.

In order to find an expression for the signal we will first consider that the changes are dominated by Γ_1. In doing so, we adopt here a different approach from that in Monteiro (1996), who consider that the dominant contribution could be isolated in the derivative of the sound speed. We do so because the effect of the ionization is better represented as a 'bump' in Γ_1 (see Figs 1 and 2), extending over a localized region of the Sun. Therefore we retain the terms for $\delta\Gamma_1$, and neglect, as a first approximation, the contributions from $\delta\rho$ and δP. In doing so we assume that the changes in the sound speed are mainly a result of the changes in the adiabatic exponent.

Now, relating δI to the change in the eigenvalue $\delta\omega$ (and using equation A1) it follows that

$$[\delta\omega]_{\Gamma_1} \equiv \frac{[\delta I]_{\Gamma_1}}{\omega\tau_{\mathrm{t}} E_o^2} \sim \frac{\omega}{2\tau_{\mathrm{t}}} \int_{\tau_a}^{\tau_b} (f_c \cos\Lambda + f_s \sin\Lambda) \frac{\delta\Gamma_1}{\Gamma_1} \mathrm{d}\tau, \tag{A17}$$

where f_s and f_c are functions obtained from adding the coefficients of $\delta\Gamma_1$ in the expressions for δB_0, δB_1, δB_2 and δB_3 (see equation A16 and equations A5–A8).

At this point we introduce an approximate description of the effect of the second ionization of helium on the adiabatic exponent. As represented in Fig. 2(b), we adopt a prescription in which the 'bump' is approximately described by its half-width β and height $\delta_{\mathrm{d}} \equiv (\delta\Gamma_1/\Gamma_1)_{\tau_{\mathrm{d}}}$, with the maximum located at τ_{d}. This corresponds to considering the following approximating simple expression for $\delta\Gamma_1$:

$$\frac{\delta\Gamma_1}{\Gamma_1} \equiv \delta_{\mathrm{d}} \begin{cases} \left(1 + \dfrac{\tau - \tau_{\mathrm{d}}}{\beta}\right), & \tau_{\mathrm{d}} - (1-\alpha)\beta \leqslant \tau \leqslant \tau_{\mathrm{d}} \\ \left(1 - \dfrac{\tau - \tau_{\mathrm{d}}}{\beta}\right), & \tau_{\mathrm{d}} \leqslant \tau \leqslant \tau_{\mathrm{d}} + (1+\alpha)\beta \\ 0, & \text{elsewhere.} \end{cases} \tag{A18}$$

The region of the ionization zone starts at $\tau_a = \tau_{\mathrm{d}} - (1-\alpha)\beta$ and finishes at $\tau_b = \tau_{\mathrm{d}} + (1+\alpha)\beta$, giving that $\tau_b - \tau_a = 2\beta$ is the width. The parameter α represents the asymmetry of the bump, and, for a first-order analysis, it does not affect the result.

We further consider that the functions f_s and f_c are slowly varying functions of the structure when compared with the size of the ionization zone ($\sim 2\beta$), and so their derivatives can be ignored in the integration. Using this approximation we can integrate equation (A17), finding that

$$[\delta\omega]_{\Gamma_1} \sim \frac{\omega}{2\tau_{\mathrm{t}}} \beta\delta_{\mathrm{d}} \left\{ \frac{\sin\left[\omega\beta(1-\triangle)^{1/2}\right]}{\omega\beta(1-\triangle)^{1/2}} \right\}^2 \times (f_c \cos\Lambda_{\mathrm{d}} + f_s \sin\Lambda_{\mathrm{d}}). \tag{A19}$$

All quantities are now evaluated at $\tau = \tau_{\mathrm{d}}$.

Taking the dominant contributions (in terms of powers of ω and derivatives of the reference structure – see CDMT for details) of the functions f_c and f_s (equation A16), we can finally write the signal as

$$[\delta\omega]_{\Gamma_1} \sim \frac{3\delta_{\mathrm{d}}}{2\tau_{\mathrm{t}}} \frac{1 - 2\triangle/3}{1-\triangle} \frac{\sin^2\left[\omega\beta(1-\triangle)^{1/2}\right]}{\omega\beta(1-\triangle)} \cos\Lambda_{\mathrm{d}}. \tag{A20}$$

This is the expression that describes the 'additional' contribution to the frequencies of oscillation ω_{nl} if the region of the second ionization of helium is present. By assuming that we have

$$\omega_{nl} \equiv [\omega_{nl}]_{\mathrm{smooth}} + [\delta\omega_{nl}]_{\Gamma_1}, \tag{A21}$$

it is now possible to try removing the smooth component, $[\omega_{nl}]_{\mathrm{smooth}}$, by adjusting the frequencies to the expression we have found for the 'periodic' component $[\delta\omega_{nl}]_{\Gamma_1}$. In doing so the parameters describing the structure of the Sun at the location τ_{d} are determined.

This paper has been typeset from a TEX/LATEX file prepared by the author.